Highlights

- Integration of empirical and analytical models in BIM for tunneling.
- Near real-time assessment of structural damage in the design environment
- Structural damage can be assessed in real-time using simulation-based meta models
- Effective visualisation of tunneling-induced risks on a City-block scale

Real-time assessment of tunnelling-induced damage to structures within the Building Information Modelling framework

Jelena Ninić[a], Ali Gamra[b], Bahman Ghiassi[a]

[a] *School of Engineering, University of Birmingham, UK*
[b] *Centre for Structural Engineering and Informatics, The University of Nottingham, UK*

Abstract

During the initial design phases of complex multi-disciplinary systems such as urban tunnelling, the appraisal of different design alternatives can ensure optimal designs in terms of costs, construction time, and safety. To enable the evaluation of a large number of design scenarios and to find an optimal solution that minimises impact of tunnelling on existing structures, the design and assessment process must be efficient, yet provide a holistic view of soil-structure interaction effects. This paper proposes an integrated tunnel design tool for the initial design phases to predict the ground settlements induced by tunnelling and building damage using empirical and analytical solutions as well as simulation-based meta models. Furthermore, visualisation of ground settlements and building damage risk is enabled by integrating empirical and analytical models within our Building Information Modelling (BIM) framework for tunnelling. This approach allows for near real-time assessment of structural damage induced by settlements with consideration of soil-structure interaction and non-linear material behaviour. Furthermore, because this approach is implemented on a BIM platform for tunnelling, first, the design can be optimised directly in the design environment, thus eliminating errors in data exchange between designers and computational analysts. Secondly, the effect of tunnelling on existing structures can be effectively visualised within the BIM by producing risk-maps and visualising the scaled deformation field, which allows for a more intuitive understanding of design actions and for collaborative design. Having a fully parametric design model and real-time predictions therefore enables the assessment and visualisation of tunneling-induced damage for large tunnel sections and multiple structures in an effective and computationally efficient way.

Keywords: Building Information Modelling, Soil-structure interaction, tunnelling, settlements, structural damage, visualisation, meta models

1. Introduction

Growing urbanization, expansion of cities and the demand for national and transnational high-speed mobility have raised the need for efficient and environmentally-friendly transport infrastructure. Besides that, due to the limited available surface space in cities, development projects often rely on underground space. To accommodate that, major urban tunneling projects have been constructed in the last few decades, e.g. Crossrail and High Speed 2 (HS2) in the UK. Despite advanced technologies used for the underground construction in these projects, existing overground structures has been significantly damaged due to tunneling-induced settlements [1; 2].

The response of existing structures to tunnelling-induced ground movement in urban tunnelling is a fully-coupled problem of tunnel-soil-structure interaction. Therefore, many design considerations such as tunnel location, existing buildings and infrastructure above and below ground, the construction method and related construction details (i.e. driving parameters), geometrical properties (e.g. depth, diameter, lining thickness), the ground behaviour and possible critical geological conditions play an important role in the selection of the optimal design solution [3]. This optimal design solution has to satisfy several design criteria, such as structural integrity and durability of the tunnel structure for demanding use for 100 years and more, the face stability during the tunnel construction, and control of tunneling-induced settlements to minimise the impact on the existing environment. To

Email address: j.ninic@bham.ac.uk (Jelena Ninić)

achieve this, analytical, empirical and numerical methods are employed to evaluate these design objectives.

1.1. Related Work

Tunneling-induced settlements depend on soil parameters, TBM operational parameters, interactions between TBM and ground, consolidation, etc. Hence, ground settlements can be determined as a function of number of different parameters. As an example, Mair et. al. [4] and Broms & Bennermark [5] describe the importance of volume loss that results from tunnel construction. The empirical approach known as "Observational Method" [6] uses the volume (or ground) loss parameter to characterise tunnel settlements. This is an empirical parameter that depends on soil conditions, tunnel configurations and the tunnelling method [3]. Furthermore, the volume loss parameter can be defined as a function of the "gap" parameter [7] or, in case of Earth Pressure Balance (EPB) shield tunnelling, as a function of volume loss at the tunnel face (V_f), around the shield (V_s), and at the tail (V_t) [8]. This parameter is then used to derive analytical expressions of surface settlements [3]. Other researchers such as Chakeri & Onver (2014) applied statistical evaluation from over 20 existing tunnelling projects to derive an empirical solution for tunnelling-induced settlements based on set from several projects and numerical models [9]. A comprehensive summary of empirical and semi-analytical methods for evaluating tunnelling-induced ground movements in sands can be found in [10].

In the presence of surface structures, the interactions between soil and structure alters the settlement induced by ground tunnelling. To relate the strain on the building to the ground settlement, certain assumptions are required. One of many approaches that simulate the interaction is the Limiting Tensile Strain Method (LTSM), a simple 2D analytical approach which represents the structure as a linear elastic beam model with its geometrical properties and stiffness for a full decoupled soil-structure analysis. Due to its simplicity, LTSM has disadvantages that may lead to a conservative outcome, in some cases underestimating the predicted outcome [11]. In the last three decades, many authors have proposed analytical solutions for prediction of tunneling-induced damage in structures [8; 12; 13; 14]. A study on the comparison of different analytical solutions for soil-structure interaction due to tunnelling can be found in [15].

To tackle the disadvantages of analytical and empirical methods, numerical models are used to evaluate a broad range of possible outcomes, including non-linear responses [16; 17]. Timoshenko beams founded on an elastic continuum half-space with rigid links have been employed to infer the maximum building strains based on a "direct strain based approach" [18]. An equivalent beam model is further proposed for the assessment of the tunneling-induced damage for masonry structures with pre-existing cracks [19]. On the other hand, extensive multi-disciplinary research has been carried out to promote the development of numerical models and design concepts to deal with the manifold complex interactions and processes in urban tunnelling [20]. As a result, sophisticated, process-oriented computational models have been developed to capture various aspects of mechanised tunnelling including Soil-Structure Interaction (SSI) [21; 22]. Advanced computational models incorporating the nonlinear behaviour of soil, building and soil-structure interaction, following a coupled or an uncoupled approach, have also been used for prediction of tunnelling or settlement-induced damage to structures [23; 24; 25; 26; 27; 28]. However, these advanced 3D computational models are usually characterised by a high degree of detail at the cost of long computation times. To address this issue, parallelisation strategies for high performance computing can be applied [29; 30].

Another alternative solution for the problem is to substitute computationally expensive simulations with surrogate models that are trained off-line [31; 21]. This technique has been recently applied to assess tunnelling-induced damage on structures [32; 33; 34]. Firstly, Obel et al. developed an approach for meta model-based prediction of non-linear structural response to tunneling-induced settlements, where two surrogate modelling approaches were investigated (response surface and neural networks) to substitute numerical models of a façade exposed to the analytically calculated surface settlements [32]. Cao et al. proposed an approach where two decoupled FE models are developed for calculation of the non-linear response of the façade and the surface settlements due to tunnel-soil-structure interactions, and then coupled using two different types of Artificial Neural Networks (ANN) in combination with Proper Orthogonal Decomposition (POD) [33] to optimise TBM parameters and

minimise the effect of tunneling to the building. The authors extended their approach to 3D building models and with consideration of polymorphic uncertainty [34].

In the last decade, for large infrastructural projects that constitute complex multidisciplinary systems, the Building Information Modeling (BIM) framework has been increasingly employed, due to a number of features related to information management, processing, visualisation, and analysis throughout the project life-cycle [35; 36]. A BIM can store geometrical-semantic data about the project such as ground, tunnels, aboveground infrastructure, and all parameters associated with these components within its repository [37]. Furthermore, BIM facilitates processing of data to generate meaningful information that can be effectively presented and visualised, and finally used for decision making support. To enable a seamless workflow, the data in a BIM is organized in an object-oriented way so that a link between objects can be established [38]. The final step in BIM system is analysis. One of the many benefits of the data obtained from a BIM is that it can be analysed using various methods that have been developed throughout the years, which can be significant when making decisions. For example, in urban tunnelling, a complex system requires sophisticated analysis to identify a viable option for the construction. BIM permits to combine complex models and effective analysis tools so that multiple scenarios can be easily evaluated, resulting in a powerful means for decision making support especially in the early design phases.

BIM for tunneling has been successfully linked to the Finite Element (FE) simulations for applications in both urban mechanized tunnelling and conventional tunnel excavation [39; 40; 41; 42; 43] Providakis et al. on the other hand used a BIM platform to process and visualise tunneling-induced settlements and risk induced to existing infrastructure based on empirical solutions [44]. Both approaches, the assessment of design alternatives in BIM based on FE simulations or empirical models, have shown promising results. However, both possess certain limitations: the empirical model applied in [44] neglects SSI effects and non-linear structural behaviour. The assessment of the tunnel design in a BIM based on FE simulations is computationally expensive and therefore can limit the number of design alternatives that can be studied. Other recently developed approaches for efficient investigation of building response to tunneling and different design alternatives are implemented as standalone tools [33; 34] and hence are missing the link to the design (e.g. BIM) software for more holistic design assessment. Therefore, in this paper, we propose a tool that uniquely and seamlessly combines BIM, computational, analytical and empirical models and surrogate modelling techniques to assess this complex engineering problem. In our approach, the use of meta models in BIM for prediction of tunnelling-induced damage risk, considering the non-linear response of structures, combined with fully parametric BIM model, allows for efficient and user-friendly investigation of different design alternatives, hence maximising the flexibility of the design, safety, and cost reduction.

1.2. Proposed concept

To enable real-time assessment of tunneling-induced damage within BIM considering both SSI and the non-linear structural response, in this paper, we propose an approach that combines a parametric BIM, Euler-Bernoulli beams on a two-parameter elastic foundations model, and simulation-based meta models for prediction of non-linear structural response (see Figure 1). Our approach is implemented as a user-friendly plug-in for industry-standard BIM design software that allows for versatility and integration of different analysis and visualisation tools. Firstly, we develop a parametric tunnel information model using state-of-the-art BIM design tools, providing a user-friendly interface that allows control of the tunnel design parameters. Secondly, we implement prediction of the the ground settlements based on the design parameters using empirical solutions [45; 9; 46; 47]. The soil-structure interaction effects between overlaying building and the tunnelling-induced settlements are evaluated using the Vlasov model [48]. Finally, we estimate the damage induced in buildings due to soil-structure interaction using simulation-based meta models. These meta models for prediction of structural damage are devised using ANNs trained with a data set created using a sophisticated FE model of masonry structure, considering non-linear material behaviour. To ensure a robust training of the data set, the process is optimised using Particle Swarm Optimisation (PSO) method. We use the numerical FE model to evaluate tunnelling-induced damage depending on a range of parameters such as building length, percentage of openings, position of building with respect to the tunnel axis, and magnitude of settlements. The structural behaviour is evaluated in terms of tensile and shear strains, and structural damage is then classified using a scale of five damage categories from “negligible”

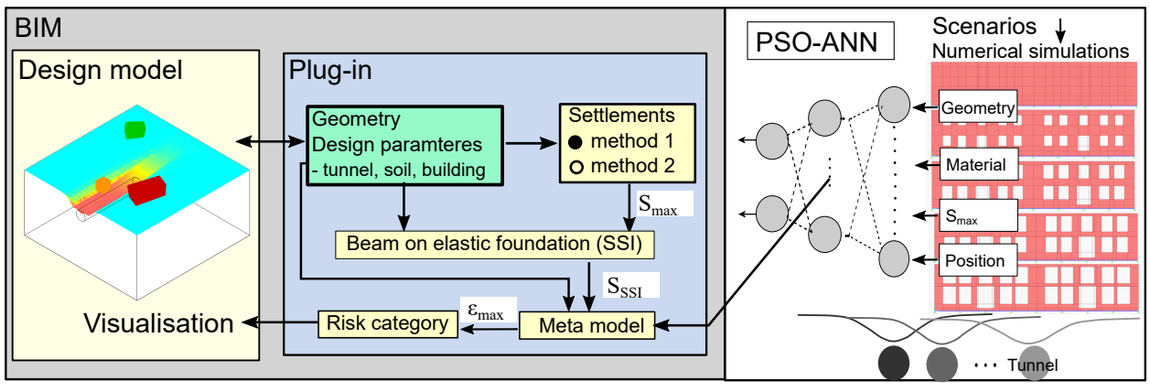

Figure 1: Concept for real-time damage assessment within BIM.

Tunnel	Soil	Building
Diameter D [m]	Geometry [m × m× m]	Height H [m]
Overburden Z_0 [m]	Young's modulus E_s [kPa]	Width W [m]
Tunnel length [m]	Cohesion C_u [kPa]	Length L [m]
Horizontal offset [m]	Poisson's ratio ν_s [-]	Young's Modulus E_b [kPa]
TBM face distance y_{face} [m]	Internal friction angle φ [°]	Poisson's ratio ν_b [-]
Face pressure [kPa]	Specific weight $[kN/m^3]$	Horizontal Offset x_b [m]
Deformation scale factor [-]	K parameter [-]	Longitudinal Offset y_b [m]

Table 1: Parameters for description of geometric-semantic BIM for tunneling.

to "severe" [12]. Trained meta models are then implemented within the BIM and used to predict the tunneling-induced damage based on the input parameters that characterise a given tunnel design and the surface settlements that result from the SSI. Finally, the resulting settlements and damage category are visualised back in the BIM model as illustrated in Figure 1 (left). The details of the methodology are described in Section 2, while the details of the implementation and verification of sub-models are presented in Section 3. Compared to existing approaches that employ complex coupled soil-structure interaction models to predict damage on structures induced by tunneling [33; 34], the proposed approach captures the same phenomena by combining simple empirical approaches, commonly adopted in practice, which gives flexibility for direct implementation in BIM software and practical application for design.

2. Methodology

In this section, we describe the methodology for integration of empirical and numerical solutions in the information model for tunneling. To this end, first we present a fully parametric tunnel model developed in BIM design software. Then, we develop an empirical solution for the 3D settlement profile and a numerical solution for soil-structure interaction based on Euler beam and Winkler model. The goal of this study is to consider complex nonliner structural response to tunneling induced settlements. Therefore, FE model described with non-linear constitutive relationship is developed, and then used for generation large data set. Finally we used ANNs to substitute computationally expensive numerical models and enable implementation of a BIM plug-in to enable real-time design and assessment of design alternatives.

2.1. Parametric information model for tunneling for visualisation of settlements

The first step in our devised methodology is to develop a fully parametric information model for tunneling within a suitable BIM environment, providing a user-friendly interface, easy control of the design parameters, and therefore efficient investigation of design scenarios. We selected the state-of-the-art Autodesk BIM design software Revit alongside with the add-on Dynamo for this purpose [49]. Dynamo is a built-in graphical algorithm editor in Revit, introducing programming aspects into the environment, which are necessary for integrative design, allowing developers to directly access the software's Application Programming Interface (API).

We create a fully parametric tunnel model, considering ground, tunnel and building components and described with the 22 parameters listed in Table 1. While a "dummy"

tunnel geometry can be modelled directly in Dynamo, the model would not carry semantic parameters, for example the diameter, which are required for analysis in a study. To tackle this issue, the tunnel and structure are created using a Revit "family" and Dynamo is used instead to provide the required parameters. A family in Revit is a class with parametric definitions and constraints, allowing the definition of specific family attributes for individual family instances (Revit objects). Then, the design model is created by inserting instances of the family with the assigned corresponding geometric-semantic parameters. This means that multiple instances can be also inserted in the same model (e.g. for multiple buildings). Figure 2 (a) shows the parametric tunnel model with all geometric parameters being retrieved and controlled in Dynamo using integer sliders.

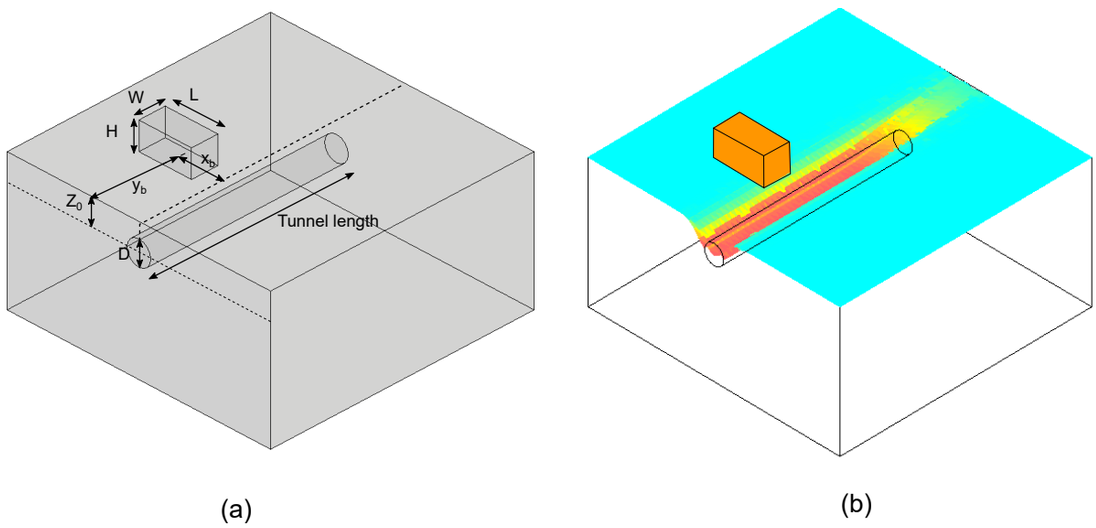

Figure 2: (a) Parametric model for tunnel, soil and building and corresponding parameters. (b) Visualisation of vertical settlements induced by tunnelling and building damage category.

2.2. Tunneling-induced settlements

The settlement trough is generally expressed in terms of a Gaussian distribution at a point source, for example, the centre of the excavation. Equation 1 shows the Gaussian function that can be applied for describing the surface settlement trough that was proposed by Peck based on studied case histories of field-observed data [50; 51]

$$S_v(x) = S_{max} \exp\left(-\frac{x^2}{2i_x^2}\right) \tag{1}$$

Where $S_v(x)$ is the ground settlement function relative to the distance from the centreline (m), S_{max} is the maximum settlement on the tunnel centreline (m), x is the perpendicular distance to the tunnel centreline (m), and i_x is the perpendicular distance from the tunnel centreline to the point of inflection point on the surface settlement trough in transverse direction (m). A typical settlement trough in the transverse direction can be seen in Figure 3. The charge of slope is at the inflection point which separates the regions between Hogging and Sagging modes as illustrated in the figure.

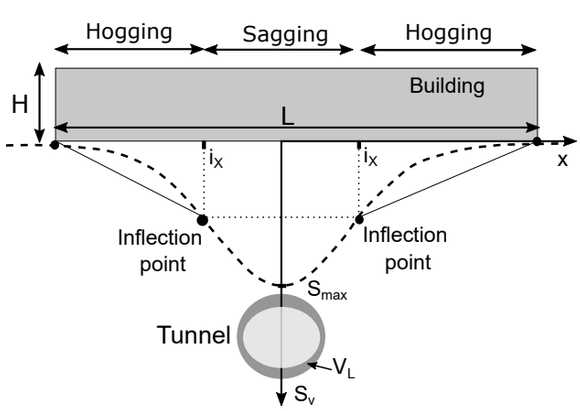

Figure 3: Description of the settlement trough, building geometry and sagging and hogging zones.

In clayey soils it is assumed that the volume of surface settlements equals the ratio between the volume of excavated soil and the theoretical volume of tunnel per unit length, which is denoted as Volume loss V_L [45]. Based on this assumption, and the assumption that the settlement profile can be described with Gaussian curve, the maximum settlement S_{max,V_L} can be calculated as:

$$S_{max,V_L} = \sqrt{\frac{\pi}{2}} \frac{V_L D^2}{4 i_x} \tag{2}$$

On the other hand, Chakeri & Onver proposed a new equation for estimating the maximum ground settlement S_{max} [9]. Employing 3D Finite Difference (FD) modelling, they derived their equation based on numerical and observed results. Using this method, which we will refer to as Chakeri & Onver method (COM), they express the maximum settlements as:

$$S_{max,COM} = AS, \qquad \text{where} \qquad A = 1.8825 \frac{D}{Z_0} \qquad \text{and}$$
$$S = 1699.2 \left(\left(\frac{\gamma Z_0 + \sigma_s - (C_u + 0.3\sigma_\tau)}{E_s} \right) (1 - \nu_s)(1 - sin\varphi) \right)^{0.8361} \tag{3}$$

Where γ is the unit weight (kN/m^3); Z_0 is the tunnel depth (m); σ_s is the surface surcharge (kPa); C_u is the cohesion (kPa); σ_τ is the required face support pressure (kPa); E_s is the Young's modulus (kPa); ν_s is the Poisson's ratio; φ is the angle of internal friction (°); and D is the tunnel diameter (m). The unit of S is assumed as mm. In our approach we allow user to select the method for calculation of the maximum settlements (equation 2 or 3), based on practical experience and available design data.

Hajjar et al. demonstrated that the geometry of the longitudinal settlement profile can be represented by the following equation [46]:

$$\frac{S_z}{S_{max}} \quad \begin{cases} \exp\left(-\dfrac{(y - y_{face} + i_y)^2}{(2 i_y^2)} \right) & \text{for} \quad y > y_{face} - i_y \\ 1 & \text{for} \quad y \leq y_{face} - i_y \end{cases} \tag{4}$$

Where y is the distance from the entrance of the tunnel, y_{face} is the distance of the face of the tunnel to the entrance of the tunnel, and i_y is the width parameter, characterising the distance between the inflection point and the nearest point with maximum settlement. Combining the transverse and longitudinal settlement profiles, we obtain the ground settlement induced by tunnelling from Equations 1, 3 and 4. This gives the following expression for the 3D settlement profile:

$$S(x, y, z) = \frac{S_z}{S_{max} \exp\left(-\frac{x^2}{2 i_x^2} \right)} \quad \begin{cases} \exp\left(-\frac{(y - y_{face} + i_y)^2}{(2 i_y^2)} \right) & \text{for} \quad y > y_{face} - i_y \\ 1 & \text{for} \quad y \leq y_{face} - i_y \end{cases} \tag{5}$$

Where S_{max} can be calculated either based on the V_L parameter using Equation 2 (settlement method 1 in Fig. 1), or with the more comprehensive approach presented in Equation 3 (settlement method 1 in Fig. 1). The resulting 3D settlement profile is shown in Figure 4. In addition to methods 1 and 2 for calculation of the settlement profiles, other solutions such as those described in [10; 52; 53] can be implemented and made available to users.

2.3. SSI model for damage assessment

After obtaining the greenfield ground settlement profile along the position of the building façade, and depending on the TBM face distance y_{face}, in the next step, we calculate the ground settlement profile that results from SSI with an existing structure on top using the Euler-Bernoulli Beam on Elastic Foundations two-parameter (EBBEF2p) model. First, the stiffness of the subgrade of the soil must be determined before it can be related to the structure. Through variational calculus, the Vlasov model parameters are expressed as:

$$k_s = \int_0^{H_s} \frac{E_s (1 - v_s)}{(1 + \nu_s)(1 - 2 v_s)} \left(\frac{d\phi}{dz} \right)^2 dz, \qquad k_1 = \int_0^{H_s} \frac{E_s}{2(1 + \nu_s)} \phi^2 dz \tag{6}$$

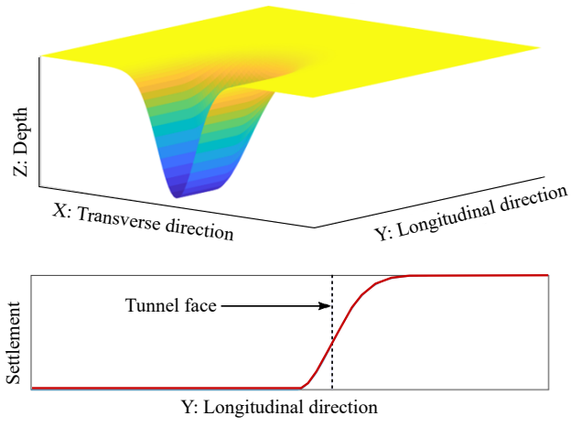

Figure 4: 3D settlement profile induced by tunneling.

Where k_s is the parameter of the elastic foundation (first subgrade), k_1 is the parameter of the rigid base (second subgrade), E_s is the deformation modulus of the soil, ν_s is the Poisson's ratio of the soil, H_s is the depth of the influence zone along the beam, and $\phi(z)$ is expressed as:

$$\phi(z) = \frac{\sinh\gamma\left(1 - \dfrac{z}{H_s}\right)}{\sinh\gamma} \tag{7}$$

Hence, a function governing the variation of the deflection $v(x, z)$ in the z-direction, which satisfies the boundary conditions of the Vlasov foundation model, is given as:

$$\left(\frac{\gamma}{H_s}\right)^2 = \frac{1 - 2v_s}{2(1 - v_s)} \cdot \frac{\int_{-\infty}^{+\infty}\left(\dfrac{dw}{dx}\right)^2 dx}{\int_{-\infty}^{+\infty} w^2 dx} \tag{8}$$

The value of γ is not known at first, thus, the parameters k_s and k_1 are determined through an iterative process, which depends on the value of the parameter γ. Therefore, in the initial step, the value of γ is approximated, and the values of k_s and k_1 are evaluated using Equation 6. Then, from the solution of the deflection of the structure, the value of γ is determined using Equation 8. In the next iteration step, the updated γ value is used again to determine new values of k_s and k_1. The process is repeated until the value of γ has converged to the given tolerance [48]. The final k_s and k_1 values are then used to compute the stiffness matrix of the elastic foundation, k_s and the rigid base, k_t. The element stiffness matrices are expressed as:

$$[k_e] = \frac{EI}{l^3}\begin{bmatrix} 12 & 6l & -12 & 6l \\ 6l & 4l^2 & -6l & 2l^2 \\ -12 & -6l & 12 & -6l \\ 6l & 2l^2 & -6l & 4l^2 \end{bmatrix} \tag{9}$$

$$[k_f] = \frac{lk_s}{420}\begin{bmatrix} 156 & 22l & 54 & -13l \\ 22l & 4l^2 & 13l & -3l^2 \\ 54 & 13l & 156 & -22l \\ -13l & -3l^2 & -22l & 4l^2 \end{bmatrix} \quad [k_t] = \frac{k_1}{30l}\begin{bmatrix} 36 & 3l & -36 & 3l \\ 3l & 4l^2 & -3l & -l^2 \\ -36 & -3l & 36 & -3l \\ 3l & -l^2 & -3l & 4l^2 \end{bmatrix} \tag{10}$$

Where $[k_e]$ is the stiffness matrix of the flexure beam element, $[k_f]$ is the stiffness matrix of the elastic foundation (first subgrade), $[k_t]$ is the stiffness matrix of the rigid base (second subgrade), and l is the length of the beam element. Equation 11 represents the relationship between all the stiffness matrices and the deflection of the structure:

$$([k_e] + [k_f] + [k_t])d_e = S_e - R_e \tag{11}$$

Where $d_e = \{w_1\,\theta_1\,w_2\,\theta_2\}^T$ are the degrees of freedom of the element, S_e are the loads $S_e = \{Q_1\,M_1\,Q_2\,M_2\}$ applied on the beam, R_e are the distributed load on the element, if

$q(x)) = q = \text{constant}$, then $R_e = \left\{ \frac{ql}{2} \frac{ql^2}{12} \frac{ql}{2} - \frac{ql^2}{12} \right\}^T$.

The formulation for Euler-Bernoulli beams on two-parameter elastic foundation presented above has been implemented in BIM as a plug-in (Dynamo node) using Python, and is used to compute the settlement profile that result from soil-structure interaction. The resulting settlement profile is then used as an input parameter for the meta model to calculate the tunneling-induced damage on structures as explained in Section 1.2. In our current implementation, the SSI effect is considered for the response of the individual buildings to tunneling-induced settlements without consideration of the mutual effects between multiple nearby buildings, which are considered negligible for detached structures.

2.4. Numerical Modelling of the non-linear structural response to Tunneling

To obtain a reliable material model, a validation process by means of numerical simulations against experimental results must be performed. The experimental work of [24] is used for this purpose. The model consists of a $1/10^{th}$ scaled masonry façade subjected to tunnelling-induced ground deformations with the material properties presented in Table 2. The SAP2000 FE package is used for the numerical simulations, adopting a macro-modelling approach, hence, allowing masonry to be modelled as a homogeneous continuum material. The isotropic Drucker-Prager model available in SAP2000 to define the uniaxial stress-strain curve is used. The uniaxial compressive behaviour is assumed to be parabolic [54] (although in the reference model [24], a linear behaviour was assumed in compression), while a linear softening in the post-peak response is used in tension. For the validation model and subsequent models, wooden lintels are inserted above the openings to prevent localized damage due to bending of the beams, and a linear elastic steel beam is placed at the bottom of the façade where the greenfield settlements are applied by means of nodal displacements in a similar fashion to the experimental setup (Figure 5). The rubber interface linking the building foundation to the steel bar used to simulate the SSI effects in the experiment was excluded from the modelling process. Hexahedral shell elements with 4 integration points are used for the mesh, and displacement control analysis is adopted with an event-to-event stepping approach to solve the nonlinear equilibrium equations. In the process, the building's self-weight is activated followed by an incremental increase of the settlements. Lastly, to determine the level of induced damage, the concept of critical strain proposed by [55] is used, and the maximum tensile strain value is measured over the length of 1 m in the facade (composed of piers, spandrels and nodes). By averaging the strain value along this distance, the averaged value is then used in Table 3 to evaluate the category of building damage.

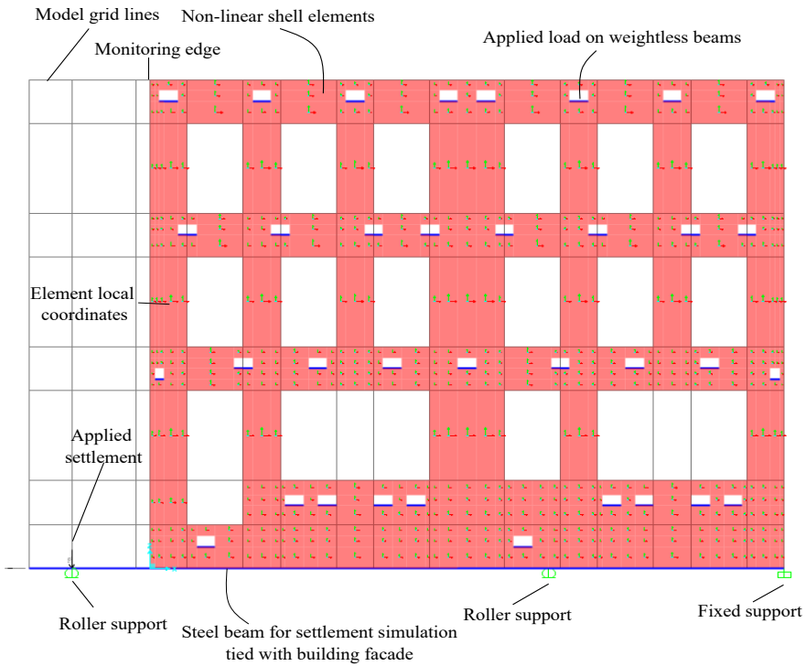

Figure 5: FEM model of the experimental set up: General configuration and boundary conditions [24].

2.5. Meta model for tunneling-induced damage

For the purpose of real-time predictions of settlement-induced damage, we employ a meta model to substitute the computational demanding numerical simulations. Concretely,

Material property	Symbol	Value (unit)
Young's modulus	E	3 (GPa)
Density	ρ	1.9×10^{-6} (kg/mm^3)
Poisson's ratio	ν	0.2
Tensile strength	f_t	0.1 (MPa)
Ultimate strain in tension*	ε_t	0.017
Compressive strength	f_c	14.1 (MPa)
Strain at peak compressive strength	ε_c	2.5×10^{-3}
Ultimate strain in compression	ε_{cu}	2.6×10^{-3}

Table 2: Material properties used for the numerical simulations based on the verification example [24]

* The strain in tension is measured according to the given value of fracture energy, $G_f = 10$ Nm/m and an elemental equivalent length, $h = 11.8$ mm which is related to the element size.

Damage category	Degree of severity	ε_{max} [%]	Colour code
0	negligible	0 – 0.05	
1	very slight	0.05 – 0.075	
2	slight	0.075 – 0.15	
3	moderate	0.15 – 0.3	
4	severe	≥ 0.3	

Table 3: Classification of building damage with the colour code for visualisation according to [56].

we instantiate a four-layer ANN (see Figure 6), taking $\boldsymbol{x}$ as input variables and the predicted tunnel-induced damage as output [57]. For the approach proposed in this paper, depending on the designed data set, the input parameters $\boldsymbol{x}$ could be any parameters used to describe building material, geometry, or position in relation to the tunnel alignment.

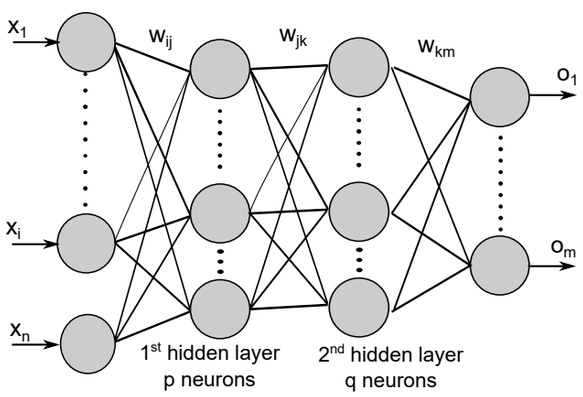

Figure 6: Structure of a 4-layer neural network for the prediction of ε_{max} of the building.

The network output (in our case, the maximum strain ε_{max}) is calculated according to Equation 12, where $\boldsymbol{w}$ are the connecting weights from the input over hidden layers 1 and 2 to the output layer, $\boldsymbol{b}$ represents the bias, $f()$ is the activation function (relu in this paper), and p and q are the number of neurons in the hidden layer:

$$o_m(x, w) = f\left(\sum_{j=1}^{q} w_{km} + f\left(\sum_{j=1}^{p} w_{jk} + b_k f\left(\sum_{i=1}^{n} w_{ij} x_i + b_j\right)\right)\right) \tag{12}$$

In the training process, the synaptic weights $\boldsymbol{w}$ and the bias $\boldsymbol{b}$ is optimised to minimise the error between ANN output $\boldsymbol{O}$ and the target $\boldsymbol{t}$.

The efficiency of the ANN training also depends on the network architecture and other training parameters such as the learning rate. To optimise the ANN training, we employ Particle Swarm Optimisation (PSO) algorithm [58]. The system is initialized with a population of random solutions and searches for optima by updating subsequent generations. Each particle belongs to a swarm and has two properties: velocity (v_{ij}) and position (x_{ij}). In each iteration, the position of the particle is updated based on the best solution (fitness), the particle-best value $x_{ij}^{p_{\text{best}}}$ and the best global value $x_{ij}^{g_{\text{best}}}$. The new velocity and position

of all particles is updated in each iteration using the following equations:

$$\begin{aligned} v_{i,j+1} &= w_{ij} + \phi_1 r_1 (x_{ij}^{p_{\text{best}}} - x_{ij}) + \phi_2 r_2 (x_{ij}^{g_{\text{best}}} - x_{ij}) \\ x_{i,j+1} &= x_{ij} + v_{i,j+1}\,. \end{aligned} \tag{13}$$

In Equation 13, r_1 and r_2 represent random numbers uniformly distributed over $[0, 1]$, and ϕ_1 and ϕ_2 are so-called cognition and social learning factors.

Prior to the training and optimisation of the ANN model, the whole data set is split and categorized into training, testing and validation sets. The ANN is trained with the training set, the fitness function of the PSO is evaluated with the testing set, and, after finding the optimal ANN model, its performance is evaluated based on the validation set. The used fitness function for the PSO is the relative Root Main Square Error (rRMSE) of the test set, where n_{test} is the number of test samples:

$$r\text{RMSE} = \sqrt{\frac{1}{n_{test}} \sum_{0}^{n_{test}} \left(\frac{o_k - t_k}{t_k} \right)^2}, \tag{14}$$

3. Implementation and testing

3.1. Algorithmic implementation

The algorithms for calculation of surface settlements, SSI, and building damage based on maximum building strains have been implemented into Dynamo as Python scripts as shown in Figure 7. The parameters used for generation of the tunnel model are also used as input variables for the implemented algorithms. Therefore, each change in the design model will automatically be applied in the analysis. Moreover, we developed a clear visualisation of the analysis results within the design model (Figure 7 right). The ground settlement profile is defined with coordinates and a smooth surface is formed by joining the points of coordinates to provide a clearer visual appearance. Then, the surfaces are associated with colours that indicate the ground settlement value (see Figure 2 (b)). Likewise, the building damage category is visualised using the colour code shown in Table 3.

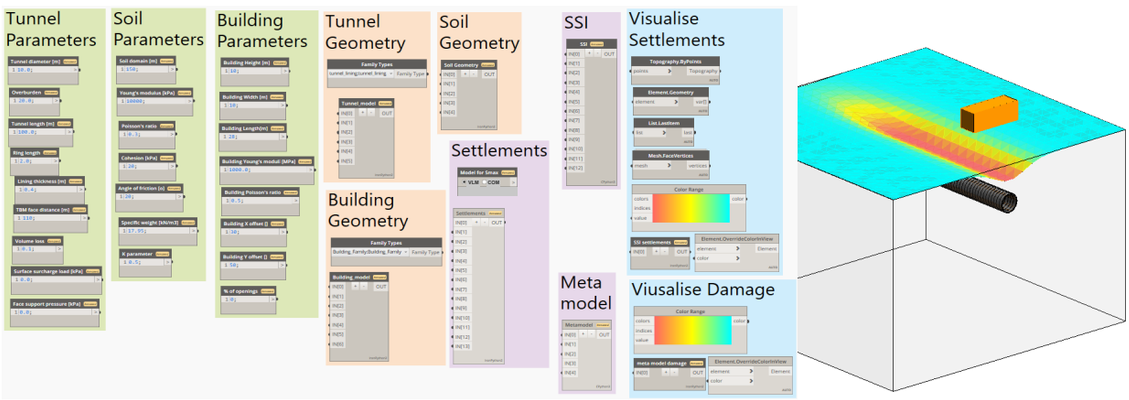

Figure 7: User interface for input of design parameters (left) and tunnel model with visualised settlements and damage category (right).

Figure 8 shows the flowchart of the implemented procedure for model generation, calculation of settlements (Section 2.2), calculation of the SSI (section 2.3), and prediction of damage category using simulation-based meta model (Sections 2.4 and 2.5) . This process begins with user input of design parameters for the soil, buildings and tunnel (geometrical and material), and then continues with the generation of BIM model and calculation of settlements based on selected empirical model. Then, the iterative process for calculation of the SSI for individual buildings begins based on inputting soil, tunnel and building parameters and an initial estimated γ value to estimate the matrices of elastic foundation and rigid base (Equation 6). At the end of each iteration, the new value of γ is compared to the initial estimated γ, and, if the value difference is within the tolerance, the iterative process ends and the new ground settlement value is output. Otherwise, the new γ is taken as the new value for the next iteration step. After the solution has converged, the results are further used for calculation of building damage category based on trained meta model and visualisation as outlined in Figure 8.

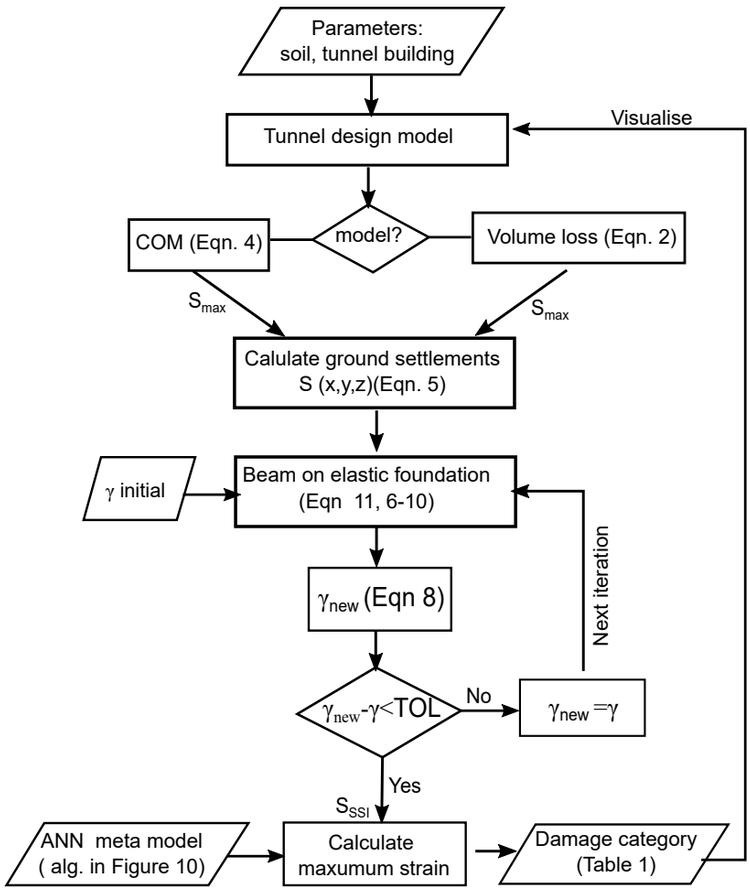

Figure 8: Algorithm for model generation and visualisation of settlements and damage category.

The algorithm for the optimised ANN training is shown in Figure 9. The meta model is trained within an iterative procedure in order to optimise ANN architecture and learning rate. The normalised data set is first split into training testing and valuation set. Then, PSO is initialised with given number of swarms and particles with its positions and velocities , that represent ANN parameters. For each particle, the ANN is trained in an iterative process based on training set and the fitness function is evaluation with testing set. After maximum number of training iteration is reached, the prediction error (rRMSE) is evaluated with validation set. This error is then used for update of particle position and optimisation of the ANN parameters. The model

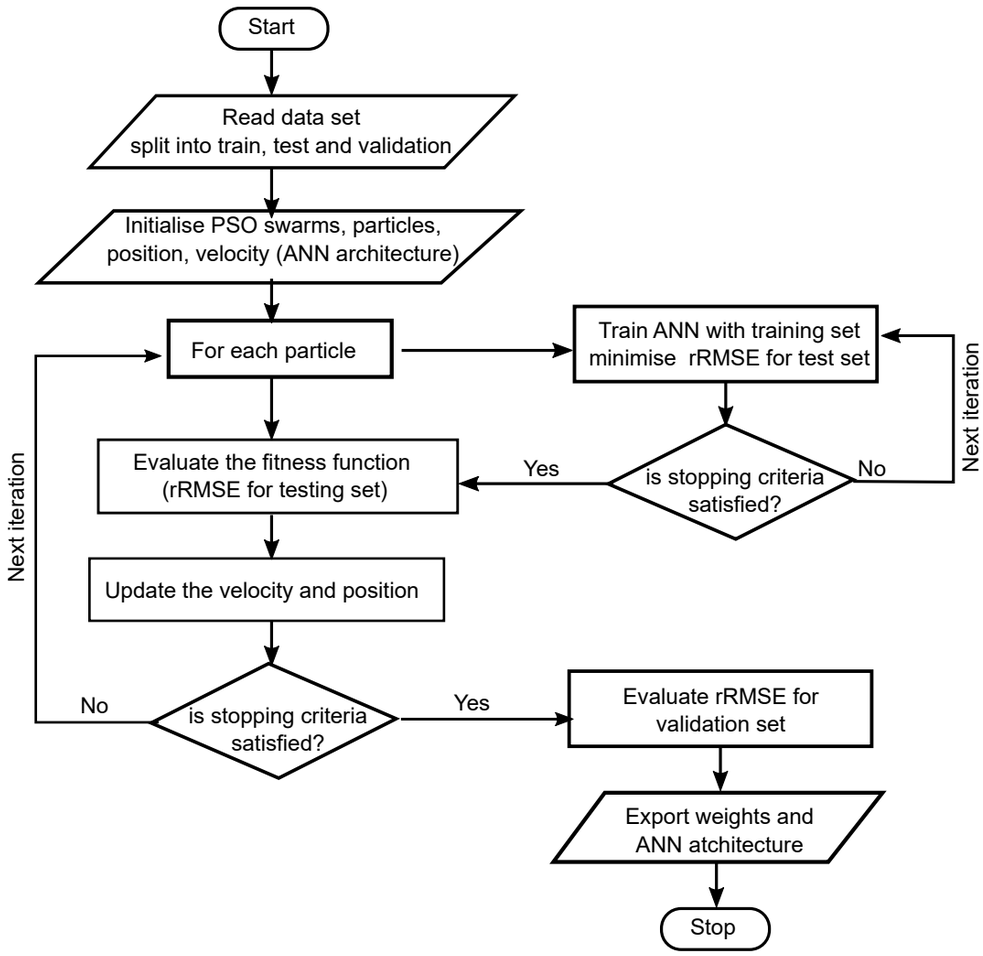

Figure 9: Algorithm for training of ANN optimised with the PSO algorithm.

3.2. Verification and testing

3.2.1. Verification of beam elastic foundations model

To verify our implementation of the iterative procedure for SSI using a modified Vlasov foundation model, an example by Teodoru [48] (see Figure 10) is compared with our implementation. Table 4 summarises the input parameters of the example.

Euler-Bernoulli Beam				**Elastic Foundation**		
Length	Width	Height	Young's modulus	Depth	Deformation modulus	Poisson's ratio
L [m]	b [m]	h [m]	E [MPa]	H [m]	Es [MPa]	ν_s
20	0.5	1	27000	5	20	0.25

Table 4: Input parameters for beam on modified Vlasov foundation, using the example [48] shown in Figure 10.

Figure 11 shows a comparison between the benchmark results of Teodoru (2009) and our implementation. The example in Figure 10 represents a model of a 20 m long beam supported by foundation and exposed to concentrated load in the middle of $P = 500\,\text{kN}$. Due to axially symmetric conditions, only one half of the model is considered. Note that Teodoru's benchmark results compare EBBEF2p and 2D FE model, which show good agreement, wheres our solution is identical to Teodoru's implementation of EBBEF2p. Therefore, the Winkler solution is an acceptable analytical method to replace 2D FEM to reduce computational cost while still producing reliable results. Our implementation gives results (red dots in Figure 11) identical to Teodoru's EBBEF2p, i.e. we have successfully verified its correctness.

To evaluate the influence of beam and soil stiffness on the settlement due to SSI, in Figure 12 we plot the deflection of the beam for beam Young's modulus varying between 27 GPa (reference value from Teodoru's example) to 1 MPa (see Figure 12 (a)) and Deformation modulus varying from 200 MPa to 2 MPa (see Figure 12 (b)). From this figure we clearly observe the effect of the SSI on the beam deflection modified settlement profile for different beam and soils stiffness.

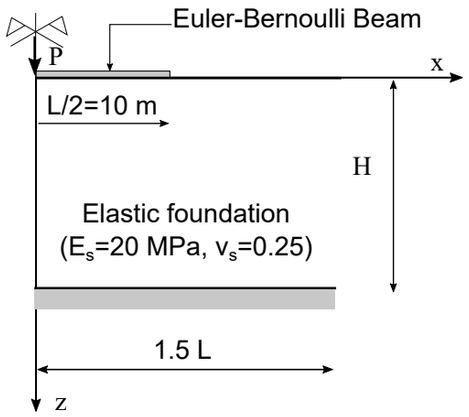

Figure 10: Beam on elastic foundation: geometry of verification example [48].

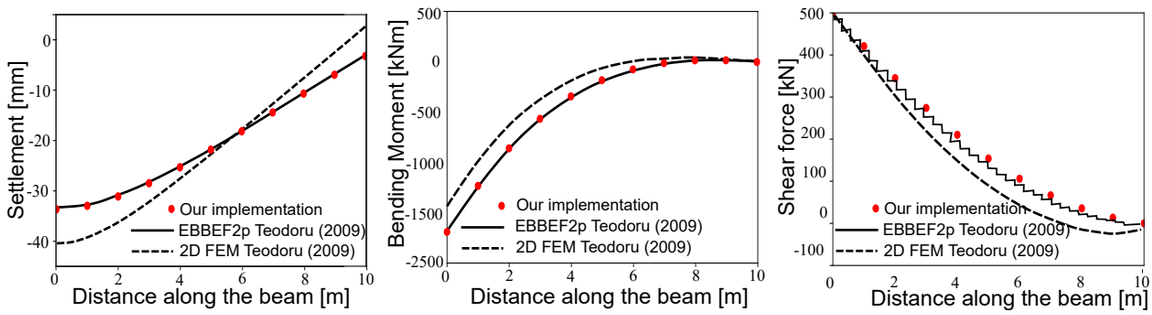

Figure 11: Comparison of settlements, bending moment and shear force. Verification between benchmark results of Teodoru [48] and this implementation.

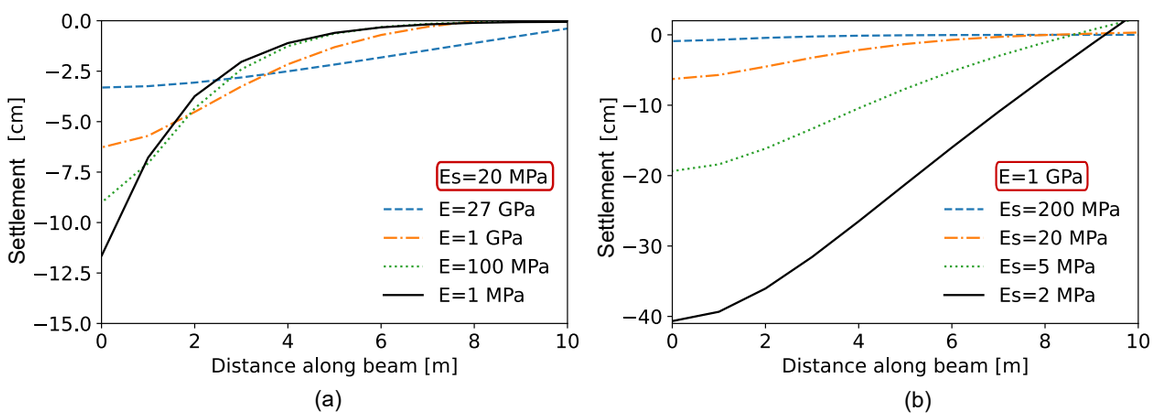

Figure 12: Comparison of settlements for variation of: (a) Beam Young's modulus E, and constant deformation modulus of $E_s = 20\,\text{MPA}$; and (b) Deformation modulus s E_s, and constant Young's modulus $E = 1\,\text{GPa}$.

3.2.2. Verification of the computational model for the predictions of damage risk

The numerical model in our implementation was able to capture the global displacements quite accurately; see Figure 14), where point B and point C are located near the top left corner of the facade and are used to monitor the vertical and horizontal movements, respectively. Furthermore, Figure 13 (left) shows the distribution of cracks in the facade cause by the settlements. By comparing it to the maximum strain values developing in the structure (Figure 13 (right)), we can conclude that the results are generally in good agreement with the reported values (Figure 13 (left)). Whilst not every crack pattern was captured, a general agreement is achieved. Hence, we have provided sufficient capability of the model to capture building deformations due to tunnelling, which can be further used for the parametric studies.

During the modelling stage, weightless steel beams were placed at the brick openings to avoid stress concentrations due to the applied point loads. The point loads were modelled at the brick openings (removed for this purpose) to account for the scaling factor. The maximum tensile strain values are used throughout the paper as a measure of developing damage. However, it is often assumed that cracks are fully formed when the maximum principle tensile strain value exceeds $2 \times \varepsilon_{tmax}$ [59].

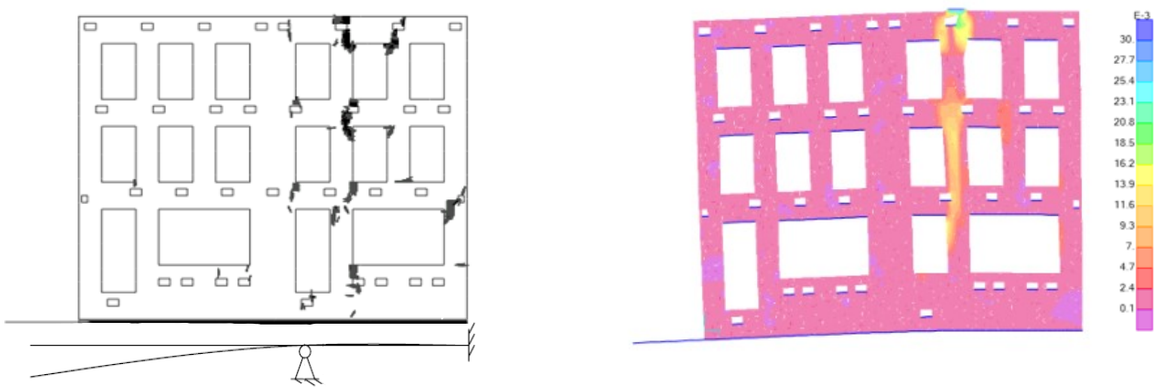

Figure 13: Developed damage on masonry facade. (left) experimental results (crack formation) [24], (right) numerical model (maximum principle tensile strain values).

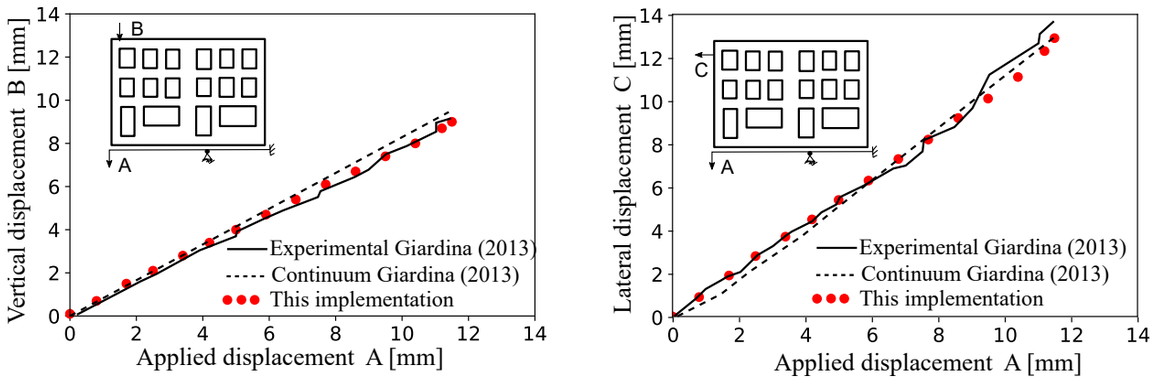

Figure 14: Verification of global behaviour for the prediction of tunnelling-induced deformations against the experimental and numerical model used in [24]. (left) Vertical displacements (Right) horizontal displacements

4. Evaluation of damage induced by tunneling within BIM

4.1. Numerical experiment for collection of data

The meta model for prediction of tunneling-induced building damage is developed following the methodology explained in Section 2.4. For a robust and a reliable meta model, a large number of FE simulations for a given range of parameters ("numerical experiment") has to be conducted to generate the data set for ANN training. To investigate various model configurations, different building geometries, material type, soil and tunnel parameters are combined to create a range of unique scenarios. For the purpose of this study, we are only addressing a few of highly influential parameters which contribute significantly in determining tunnelling-induced building damage. These parameters are carefully selected based on the information found in the literature (see Table 5). As a result a total number of 360 simulations are performed and used for the training, testing and validation of the meta model.

Parameters	Range	Increment
Percentage of openings [%]	0-50	10
Distance of building centre from tunnel centreline x_b [D]	0-4	1
Maximum settlement S_{max} [mm]	15-35	10
Building length [m]	28-40	4

Table 5: Input parameters ranges used to generate data sets for meta model training.

An illustration of the different model parameters can be seen in Figure 15. These scenarios compromise different building lengths, % of openings, magnitude of maximum settlement, and building distance using a full factorial sampling strategy to ensure coverage of all possible combinations. The settlement profile for given S_{max}, estimated with EBBEF2p for the corresponding scenario, is applied at all nodes of the facade model by applying linear interpolation between the nodes [33].

Examples of simulation models for the failure modes are shown in Figures 16 and 17. In Figure 16, we illustrate that for different building configurations, different failure mechanisms occur, as the maximum principle tensile strains tend to localize towards the weakest parts of

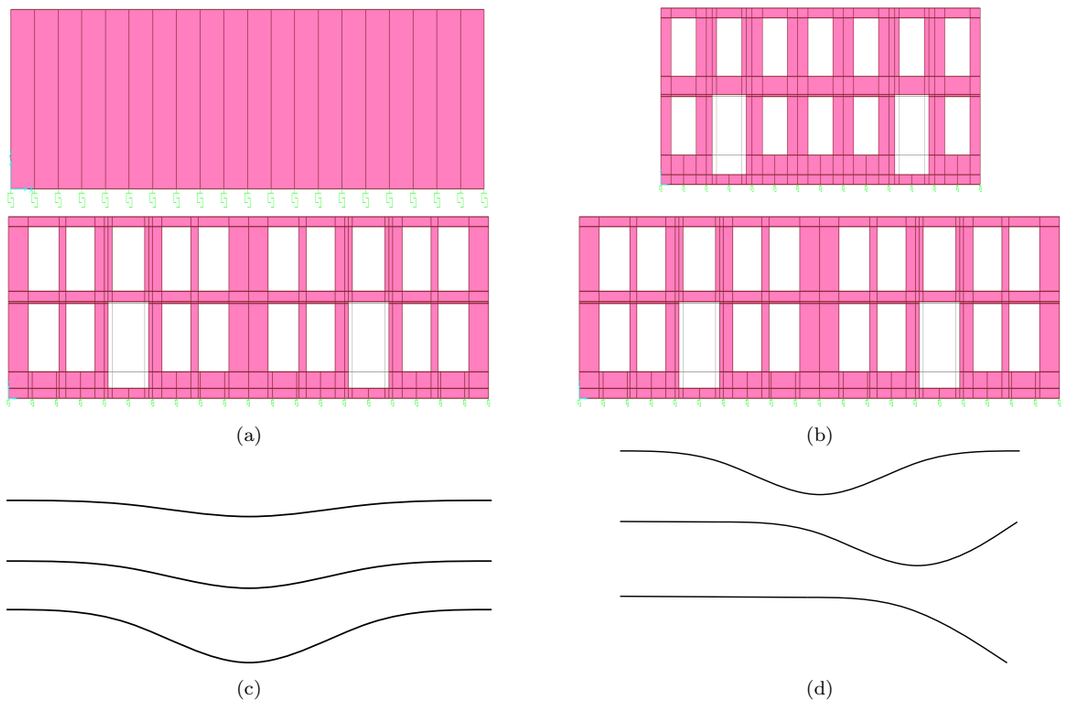

Figure 15: Model parameters adopted for the parametric studies (a) opening rate (b) building length (c) maximum settlement (d) ground location (building distance). Settlement profiles not to scale and for illustrative purposes only.

the structure. For a wall without any openings (Figure 16a), vertical cracks are more likely to occur and their locations depend on the building location with respect to the tunnel centreline. Similarly, cracks propagate vertically through the structural elements in buildings with higher opening ratio (i.e. 10%) (Figure 16b) whilst located at hogging regions. This is because of the bending effect causing the structural elements (spandrels) to absorb high tensile strains leading to localized failure. On the other hand, if buildings with large opening ratio (i.e. 30%) are located at sagging regions, piers are subjected to significant shear forces leading to diagonal cracking due to local deformation caused by the vertical displacement as well as the restraint effect caused by the foundation.

In Figure 17 the effect of increasing in the input parameter on the final response of buildings to settlements is illustrated. Figure 17a shows the effect of increased opening ratio. According to [56], increased opening ratios induce shear failure; here, the failure is observed to be transiting from vertical cracking (no openings) to diagonal cracking in the piers (with openings). Figure 17d shows a shift in the damage location and a change in the failure modes and deformed shape. This confirms that the building location has a significant effect on the settlement-induced damages and is in accordance with previous work such as [60]. In Figures 17b & 17c, the effects of increasing the length and maximum settlement are presented. The maximum settlement is most certainly a straightforward explanation in this case and in all studied cases in this study, where higher settlements induce higher levels of tensile strains at specified regions. Due to foundation restrictions particularly above sagging zones, higher shear failures are observed with the increase in building length.

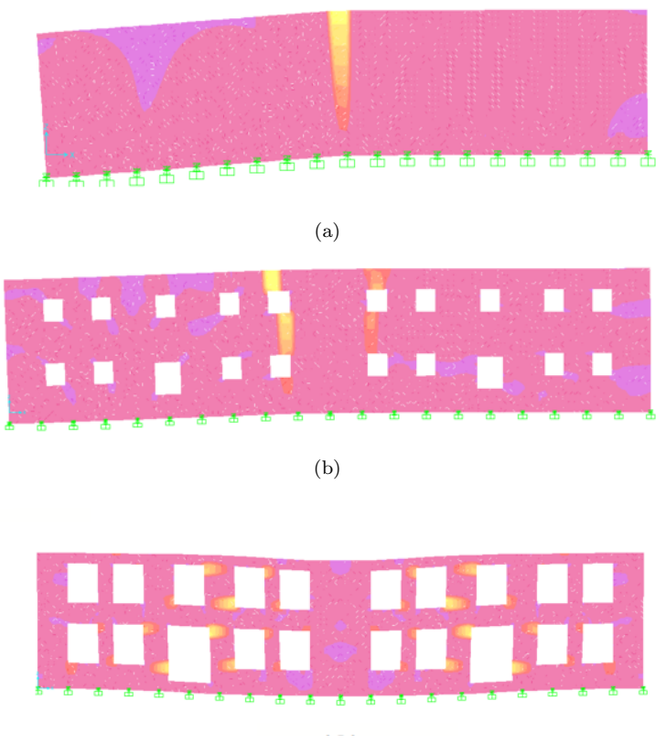

Figure 16: Failure modes of different configurations. (a) vertical crack developing due to bending (b) vertical cracks propagating through the openings (spandrel failure) (c) diagonal cracking developing in the piers due to shear failure (contours of the maximum principle tensile strain).

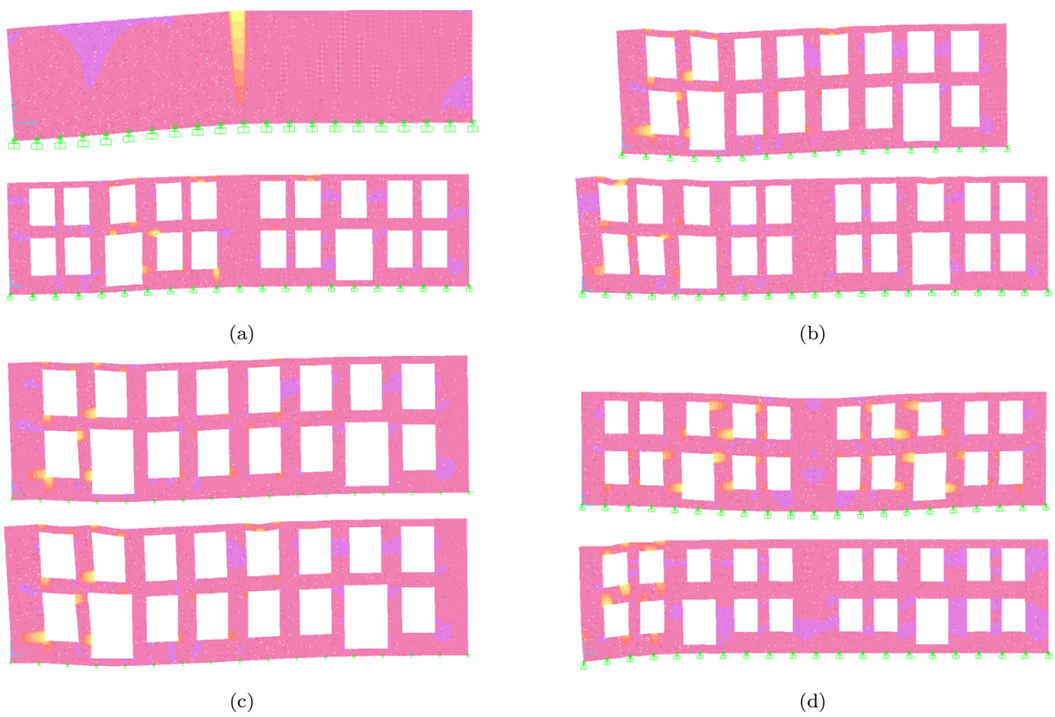

Figure 17: Illustration of the failure mode of different scenarios based on the (a) percentage of openings in the structure; (b) length of the building; (c) magnitude of settlements; (d) offset of structure from the tunnel center-line.

4.2. ANN training

After collection of data, each pair of parameter combinations (input parameters for buildings: building length, percentage of openings, distance from tunnel center-line, and maximum settlement) and level of building damage are organized, so that for each combination of parameters a specific level of building damage is assigned. In this case, 360 sets of data are obtained. For the training of meta model the data is split for training based on the algorithm presented in Section 2.5, testing and validation of the algorithm. A suitable split in this case would be 80% (288 cases) training 10% (36) testing and 10% (36) validation. The accuracy

of the model is obtained in terms of the relative root mean square error (rRMSE).

To improve training, the numerical simulation data is first normalized using the following equation:

$$V_{norm} = \frac{V - V_{min}}{V_{max} - V_{min}} \cdot (V'_{max} - V'_{min}) + V'_{min} \tag{15}$$

Where V_{norm} is the normalized value, V_{max} and V_{min} are the maximum and minimum value of the variable V.V'_{max} and V'_{min} are the maximum and minimal values of the variable V after normalization, defined as 0.1 and 0.9. The normalised data set is trained using the algorithm shown in Figure 9.

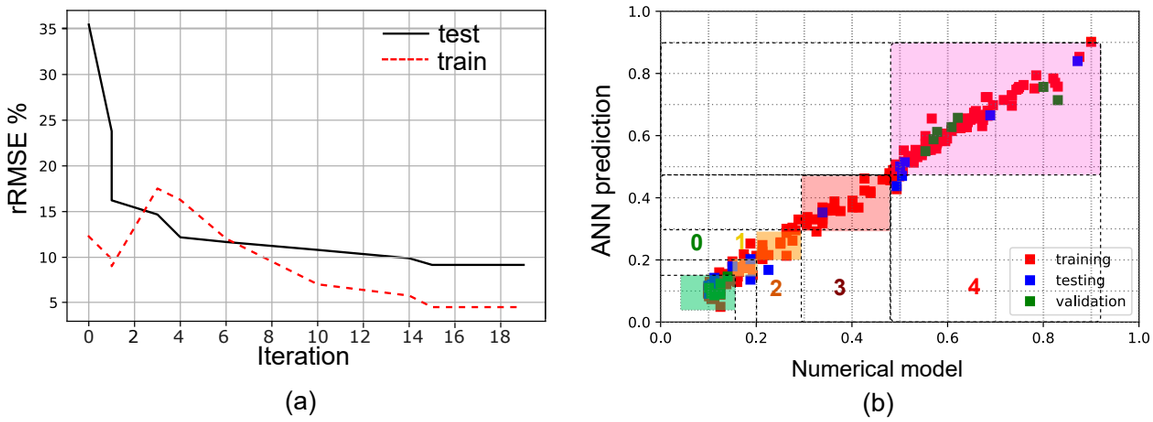

Figure 18: (a) Convergence of PSO algorithm for ANN training; (b) Comparison between numerical model and meta model prediction of tunneling-induced damage.

Figure 18(a) shows the convergence of PSO for ANN training for optimisation of the ANN parameters learning rate and number of neurons in the hidden layers. The ANN parameters are optimised to minimise the fitness (rRMSE) of the testing set and therefore avoid overfitting (an example for which can be seen in the first iteration step). The iterative process converges after fifteen steps. Figure 18(b) shows a comparison between the numerical model results and the prediction of trained ANN for the training, testing, and validation set, with rRMSE of 4.47 %, 9.09 %, and 6.96% , respectively. The damage categories that correspond to the predicted values of maximum strains are highlighted in Figure 18 (b), and it is shown that, even with a relatively high training error, the category of damage is predicted with high confidence.

4.3. Prediction of damage risk in BIM based on meta models

After training the data set for prediction of damage based on the ranges of parameters given in Table 5, a custom node is implemented using the Dynamo API. The node reads the trained synaptic weights and ANN architecture and performs forward calculation to predict the damage risk based on the model parameters. The settlement at the foundation level of the building is predicted by the beam on elastic foundation algorithm in Figure 8, without considering mutual interactions of multiple buildings. The bending stiffness of the equivalent beam depends on the percentage of opening in the walls. Therefore, to consider this in our SSI model, the modified elastic stiffness of the building is calculated using the approach of [61], considering a simply supported beam with uniform loading:

$$E_{eq} = \frac{M \cdot L^2}{8 \cdot I \cdot \delta_b} \qquad \text{where} \qquad M = \frac{\sigma_{max} \cdot I}{0.5 \cdot H} \tag{16}$$

where, E_{eq} is the equivalent stiffness [MPa], M is the bending moment [N.mm], L is the length of the building [mm], I is the moment of inertia [mm^4], δ_b is the maximum settlement at mid point [mm], σ_{max} is the maximum stress along the building width [MPa] for the respective percentage of the openings and length, and H is the building height [mm]. This elastic stiffness is used as an input parameter for the beam on elastic foundation model.

The meta model is implemented in the design tool's API and can be used for prediction of the damage category for the given building geometry and settlements resulting from the SSI. Figure 19 shows examples of meta model predictions of building damage, illustrated in the colour coding from Table 3, for structures with different lengths, % of opening and distance from tunnel centreline exposed to tunneling-induced settlements. Usually, the further the structure is from the tunnel centreline, the lower damage occurs. However, this is sometimes

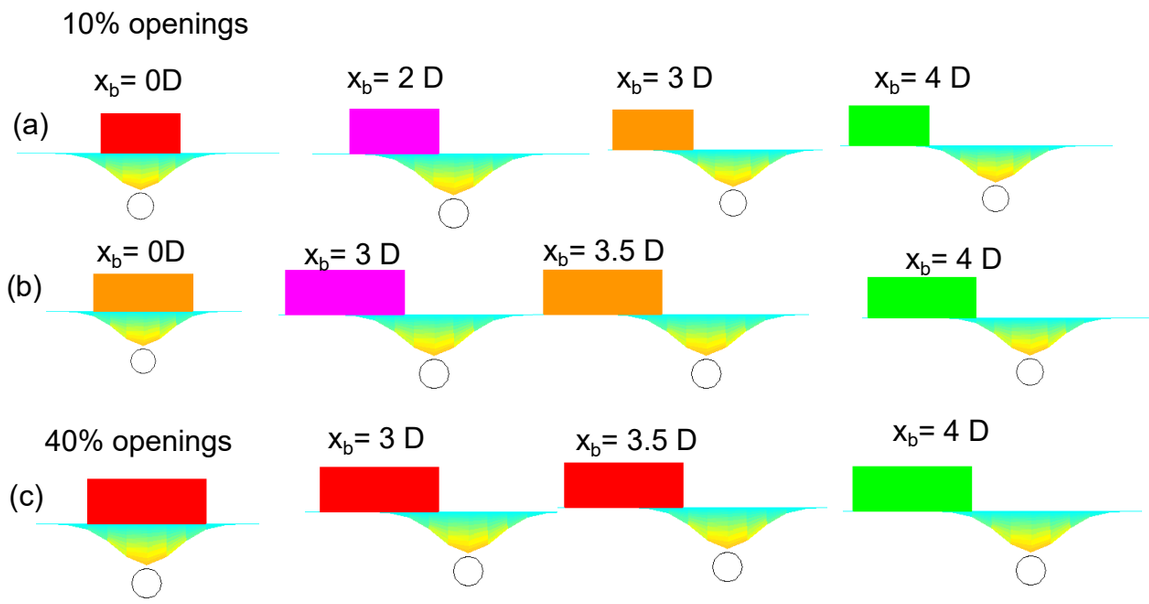

Figure 19: Prediction of tunneling-induced damage category based on meta model for different positions of the buildings (x_b), building lengths L and percentage of openings in buildings O_b. (a) $L = 30\,\text{m}$ and O_b =10%; (b) $L = 40\,\text{m}$ and O_b =10%;(c) $L = 40\,\text{m}$ and O_b =40%.

not the case when the structure is either in pure sagging or pure hogging modes. This is because the structure behaves differently in those regions, where the percentage of opening plays a vital role in the determination of the induced damage. For example, if the structure is in hogging mode and a roof spandrel fails affecting the overall relative deflection, the damage is considered to be critical, while the structure can have a different failure mode in case of sagging where a spandrel is not the weaker element. This prediction matches the output of the FE simulation, due to suitable meta model training, meaning that the complex deformation mechanisms are accurately captured and predicted in the BIM model.

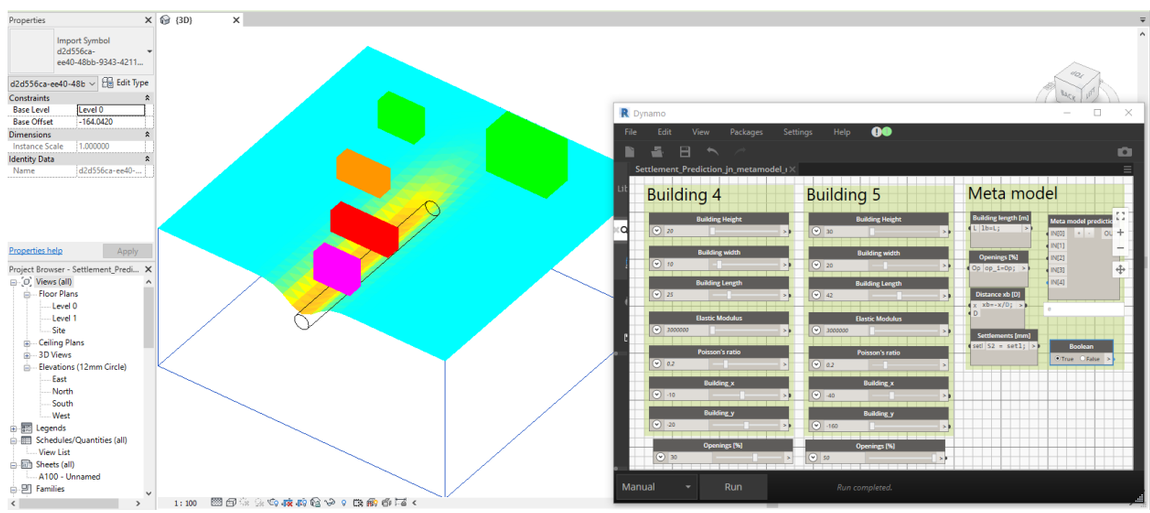

Figure 20: Real-time prediction of tunneling-induced damage risk for multiple buildings in the design environment.

Having a fully parametric model for tunneling (soil, tunnel, building) and an automatic workflow for prediction of settlements, assessment of SSI based on EBBEF2p model, and assessment of damage risk based on the trained meta model, we can generate design models, assess multiple buildings at the same time, and visualise the results in the design environment as shown in Figure 20. Most importantly, this procedure is executed in near real-time (within seconds) while considering soil-structure interaction and the non-linear response of masonry structures to settlements. This shows that the combination of empirical, numerical and meta models is a powerful tool for quick and efficient investigation of design alternatives directly in design tools. Having a user-friendly environment further enables designers to easily investigate, evaluate and optimise a design, without having expert knowledge about the implemented methodology. The visualisation of the settlements and induced risk category is intuitive, therefore, can be efficiently used to present the results to non-experts or support

decision making process.

5. Conclusions

In this paper, we propose a holistic approach for the assessment of tunneling-induced settlements and the damage risk category of structures affected by tunneling. Our methodology, which combines empirical, numerical and simulation-based meta models, is implemented in a state-of-the art design tool. This enables the user to manipulate the design or models easily and effectively optimise the design directly in a BIM environment.

The efficient investigation of the design scenarios is enabled by implementing methods for parametric design and real-time assessment. The design model is implemented utilising a BIM object-oriented parametric 3D solid geometric semantic representation. For each tunnel component (tunnel, soil, buildings), a template is created using Revit families, and the design model is then generated from instances of those families with parameters assigned through the user interface. Our methodology for the assessment of SSI and damage category combines i) an empirical solution for prediction of the 3D ground settlement field, ii) the Euler-Bernoulli beam two-parameter elastic foundations model, and iii) simulation-based meta model for prediction of the damage category. The numerical model for generation of the data set is implemented in SAP200, considering a non-linear material model for masonry. The meta models are trained with an PSO-ANN algorithm developed for robust and efficient training.

Furthermore, the models implemented in our methodology for both the beam on elastic foundation model and the numerical model for masonry structure exposed to settlements are validated and verified against models and data available in the literature. Both verification examples show excellent agreement with the reference data. Moreover, the trained ANN model also has high precision for predicting the damage risk category. Hence, the overall methodology and its implementation that combines these verified sub-components leads to high confidence in the prediction of the effect of tunneling. Thus, the proposed tool can be applied to reliably support decision making during the design phase, saving time and cost, which was our initial goal for creating such a tool in a BIM process. Below, we summarise the major contribution of the work presented in this paper:

- **Real-time prediction of complex SSI including non-linear structural response**: we propose a method for prediction of tunneling-induced damage risk that takes into consideration both the interaction of the building with the soil and the non-linear response of structures. Combining the empirical model for predictions of settlements, the beam on elastic foundations for prediction of SSI, and the meta model that accounts for non-linear structural behaviour and different failure modes, we developed a method that allows for near-instant prediction, yet capturing very complex phenomena.
- **Use of meta models in BIM for prediction of complex phenomena**: We generate meta models based on sophisticated numerical simulations that capture the complex non-linear behavior of a structure exposed to tunneling, which can result in several different failure modes depending on the building geometry and position w.r.t. the tunnel the and magnitude of settlements. Yet, the trained meta models predict all the dependencies between these design variables and the effect to structures with high accuracy. Moreover, such meta models can be easily and efficiently implemented in a design environment like BIM.
- **Assessment of structural response in BIM**: Our approach allows to generate the design in a BIM environment and directly perform the analysis and effectively visualise the soil-structure interaction effects without leaving the software. Firstly, performing the analysis directly in the BIM design environment eliminates human error for manually reading data and generating models. Secondly, the analysis results are visualised within the BIM to enable comprehensive, intuitive and quick understanding of effects of design actions on the stability and safety of the tunnel and the existing environment.
- **Assessment of the SSI for City-blocks**: Having real-time predictions combined with a fully parametric BIM model, we are able to analyse the effects of tunnels on multiple buildings instantaneously. This shows that the proposed tool can can be employed for the efficient analysis of large tunnel sections.

In the current approach, the meta model for prediction of the damage induced by settlements is established based on a limited data set generated with consideration of only four design parameters. In future research, we plan to generate a more comprehensive data set, considering geometric and semantic parameters (e.g. building shape and size, material type, and material properties). This will allow to predict the expected damage category with higher accuracy for City-blocks with very diverse structures. Furthermore, for the current implementation, we only considered 2D models for the façades on strip foundations. In future extensions of our work, we will develop meta models and adjust the existing concept to account for 3D buildings with arbitrary orientation w.r.t. the tunnel alignment. To allow for that, we can implement alternative solutions for more accurate representation of SSI by consideration of shear flexibility with Timoshenko beams using a continuum approach [62; 63]. Moreover, to account for multi-layered soil, the SSI model can be seamlessly extended [64]. However, to consider different types of foundations such as plate foundations, due to the complexity of the problem, a new strategy for SSI must be adopted. For example, we either could implement the SSI model in our FE model of the building [65], or alternatively evaluate the SSI based on advanced numerical simulation models for tunnel-soil-building similar to [34]. Finally, to increase the level of automation, we aim to develop a method for automatic generation of approximated building geometry and establishment of a parametric City-model suitable for the analysis from available CAD data.

References

[1] M. J. DeJong, G. Giardina, B. Chalmers, D. Lazarus, D. Ashworth, R. J. Mair, Impact of the crossrail tunnelling project on masonry buildings with shallow foundations, Proceedings of the Institution of Civil Engineers-Geotechnical Engineering 172 (5) (2019) 402–416.

[2] P. Milillo, G. Giardina, M. J. DeJong, D. Perissin, G. Milillo, Multi-temporal InSAR structural damage assessment: The London crossrail case study, Remote Sensing 10 (2) (2018) 287.

[3] N. Loganathan, H. G. Poulos, Analytical prediction for tunneling-induced ground movements in clays, Journal of Geotechnical and Geoenvironmental Engineering 124 (1998). doi:https://doi-org.ezproxy.nottingham.ac.uk/10.1061/(ASCE)1090-0241(1998)124:9(846).

[4] R. Mair, R. N. Taylor, A. Bracegirdle, Sub-surface settlement profiles above tunnels in clays, Geotechnik 43 (2) (1993) 315–320.

[5] B. Broms, H. Bennermark, Stability of clay at vertical openings, Journal of Soil Mechanics & Foundations Div 93 (1967) 71–94.

[6] A. J. Powderham, An overview of the observational method: development in cut and cover and bored tunnelling projects, Géotechnique 44 (4) (1994) 619–636. arXiv:https://doi.org/10.1680/geot.1994.44.4.619, doi:10.1680/geot.1994.44.4.619.

[7] K. M. Lee, R. K. Rowe, K. Y. Lo, Subsidence owing to tunnelling. i. estimating the gap parameter, Canadian Geotechnical Journal 29 (6) (1992) 929–940. arXiv:https://doi.org/10.1139/t92-104, doi:10.1139/t92-104.

[8] J. Franzius, Behaviour of buildings due to tunnel induced subsidence, Ph.D. thesis, Imperial Collece of Science, Technology and Medicine, University of London (2003).

[9] H. Chakeri, B. Ünver, A new equation for estimating the maximum surface settlement above tunnels excavated in soft ground, Environmental Earth Sciences 71 (2013) 3195–3210. doi:10.1007/s12665-013-2707-2.

[10] A. Franza, A. M. Marshall, Empirical and semi-analytical methods for evaluating tunnelling-induced ground movements in sands, Tunnelling and Underground Space Technology 88 (2019) 47 – 62. doi:https://doi.org/10.1016/j.tust.2019.02.016.

[11] J. Burland, C. Wroth, Settlement of buildings and associated damage, in: Conference on Settlement of Structures, 1975.

[12] M. D. Boscardin, E. J. Cording, Building response to excavation-induced settlement, Journal of Geotechnical Engineering 115 (1) (1989) 1–21. doi:10.1061/(ASCE)0733-9410(1989)115:1(1).

[13] D. Potts, T. Addenbrooke, A structure's influence on tunnelling-induced ground movements., Proceedings of the ICE-Geotechnical Engineering 125 (2) (1997) 109–125.

[14] K. Goh, R. Mair, Building damage assessment for deep excavations in singapore and the influence of building stiffness, Geotechnical Engineering 42 (2011) 1–12.

[15] G. Giardina, M. J. DeJong, B. Chalmers, B. Ormond, R. J. Mair, A comparison of current analytical methods for predicting soil-structure interaction due to tunnelling, Tunnelling and Underground Space Technology 79 (2018) 319 – 335. doi:https://doi.org/10.1016/j.tust.2018.04.013.

[16] J. Burland, J. Standing, F. Jardine, Assessing the risk of building damage due to tunnelling - lessons from the Jubilee Line Extension, London, in: Proceedings of the 2nd International Conference on Soil Structure Interaction in Civil Engineering, Zurich, 2002, pp. 11–38.

[17] D. Potts, L. Zdravkovic, Finite element analysis in geotechnical engineering: application, 2001.

[18] A. Franza, S. Acikgoz, M. J. DeJong, Timoshenko beam models for the coupled analysis of building response to tunnelling, Tunnelling and Underground Space Technology 96 (2020) 103160. doi:https://doi.org/10.1016/j.tust.2019.103160.

[19] S. Acikgoz, A. Franza, M. J. DeJong, R. Mair, Cracked equivalent beam models for assessing tunneling-induced damage in masonry buildings, Journal of Geotechnical and Geoenvironmental Engineering 147 (2) (2021) 04020167. doi:10.1061/(ASCE)GT.1943-5606.0002443.

[20] G. Meschke, From advance exploration to real time steering of TBMs: A review on pertinent research in the Collaborative Research Center "Interaction Modeling in Mechanized Tunneling", Underground Space 3 (1) (2018) 1 – 20, computational Methods in Mechanized Tunneling. doi:https://doi.org/10.1016/j.undsp.2018.01.002.

[21] J. Ninic, S. Freitag, G. Meschke, A hybrid finite element and surrogate modelling approach for simulation and monitoring supported tbm steering, Tunnelling and Underground Space Technology, 63 (2017) 12–28.

[22] J. Ninic, J. Stascheit, G. Meschke, Beam-solid contact formulation for finite element analysis of pile-soil interaction with arbitrary discretization, International Journal for Numerical and Analytical Methods in Geomechanics 38 (14) (2014) 1453–1476.

[23] M. Son, C. E. J, Estimation of building damage due to excavation-induced ground movements, Journal of Geotechnical and Geoenvironmental Engineering 131 (2) (2005) 167–177.

[24] G. Giardina, Modelling of settlement induced building damage, Delft University of Technology, TU Delft (2013).

[25] W. N. Yiu, H. J. Burd, C. M. Martin, Finite-element modelling for the assessment of tunnel–induced damage to a masonry building, Géotechnique 67 (9) (2017) 780–794. doi:10.1680/jgeot.sip17.P.249.

[26] V. Fargnoli, C. Gragnano, D. Boldini, A. Amorosi, 3d numerical modelling of soil–structure interaction during epb tunnelling, Géotechnique 65 (1) (2015) 23–37. doi:10.1680/geot.14.P.091.

[27] D. Boldini, N. Losacco, S. Bertolin, A. Amorosi, Finite element modelling of tunnelling-induced displacements on framed structures, Tunnelling and Underground Space Technology 80 (2018) 222 – 231. doi:https://doi.org/10.1016/j.tust.2018.06.019.

[28] S. Miliziano, A. de Lillis, Predicted and observed settlements induced by the mechanized tunnel excavation of metro line c near s. giovanni station in rome, Tunnelling and Underground Space Technology 86 (2019) 236 – 246. doi:https://doi.org/10.1016/j.tust.2019.01.022.

[29] H.-G. Bui, G. Meschke, A parallelization strategy for hydro-mechanically coupled mechanized tunneling simulations, Computers and Geotechnics 120 (2020) 103378. doi:https://doi.org/10.1016/j.compgeo.2019.103378.

[30] J. Ninic, H. G. Bui, C. Koch, G. Meschke, Computationally efficient simulation in urban mechanized tunneling based on multilevel bim models, Journal of Computing in Civil Engineering 33 (2019) 04019007. doi:10.1061/(ASCE)CP.1943-5487.0000822.

[31] S. Freitag, B. Cao, J. Ninic, G. Meschke, Recurrent neural networks and proper orthogonal decomposition with interval data for real-time predictions of mechanised tunnelling processes, Computers & Structures 207 (2018) 258 – 273, cIVIL-COMP 2017. doi:https://doi.org/10.1016/j.compstruc.2017.03.020.

[32] M. Obel, M. A. Ahrens, P. Mark, Metamodel-based prediction of structural damages due to tunneling-induced settlements, ASCE-ASME Journal of Risk and Uncertainty in Engineering Systems, Part A: Civil Engineering 6 (4) (2020) 04020044. arXiv:https://ascelibrary.org/doi/pdf/10.1061/AJRUA6.0001092, doi:10.1061/AJRUA6.0001092.
URL https://ascelibrary.org/doi/abs/10.1061/AJRUA6.0001092

[33] B. Cao, M. Obel, S. Freitag, P. Mark, G. Meschke, Artificial neural network surrogate modelling for real-time predictions and control of building damage during mechanised tunnelling, Advances in Engineering Software 149 (2020) 102869. doi:https://doi.org/10.1016/j.advengsoft.2020.102869.

[34] B. T. Cao, M. Obel, S. Freitag, L. Heußner, G. Meschke, P. Mark, Real-time risk assessment of tunneling-induced building damage considering polymorphic uncertainty, ASCE-ASME Journal of Risk and Uncertainty in Engineering Systems, Part A: Civil Engineering 8 (1) (2022) 04021069. arXiv:https://ascelibrary.org/doi/pdf/10.1061/AJRUA6.0001192, doi:10.1061/AJRUA6.0001192.

[35] S. Smith, Building information modelling: moving Crossrail, UK, forward, Proceedings of the Institution of Civil Engineers - Management, Procurement and Law 167 (2014) 141–151.

[36] J. Daller, M. Zibert, C. Exinger, M. Lah, Implementation of BIM in the tunnel design – engineering consultant's aspect, Geomechanics and Tunnelling 9 (2016) 674–683.

[37] C. Koch, A. Vonthron, M. König, A tunnel information modelling framework to support management, simulations and visualisations in mechanised tunnelling projects, Automation in Construction 83 (2017) 78–90.

[38] C. Eastman, P. Teicholz, R. Sacks, K. Liston, BIM handbook: A guide to Building Information Modeling for owners, managers, designers, engineers, and contractors, Wiley & Sons, 2008. doi:10.1002/9780470261309.

[39] J. Ninic, C. Koch, J. Stascheit, An integrated platform for design and numerical analysis of shield tunnelling processes on different levels of detail, Advances in Engineering Software 112 (2017) 165–179.

[40] J. Ninić, C. Koch, A. Vonthron, W. Tizani, M. König, Integrated parametric multi-level information and numerical modelling of mechanised tunnelling projects, Advanced Engineering Informatics 43 (2020) 101011. doi:https://doi.org/10.1016/j.aei.2019.101011.

[41] A. Alsahly, F. Hegemann, M. König, G. Meschke, Integrated bim-to-fem approach in mechanised tunnelling, Geomechanics and Tunnelling 13 (2) (2020) 212–220. arXiv:https://onlinelibrary.wiley.com/doi/pdf/10.1002/geot.202000002, doi:10.1002/geot.202000002.

[42] J. Ninic, A. Alsahly, A. Vonthron, H.-G. Bui, C. Koch, M. König, G. Meschke, From digital models to numerical analysis for mechanised tunnelling: A fully automated design-through-analysis workflow, Tunnelling and Underground Space Technology 107 (2021) 103622. doi:https://doi.org/10.1016/j.tust.2020.103622.

[43] S. Fabozzi, S. A. Biancardo, R. Veropalumbo, E. Bilotta, I-bim based approach for geotechnical and numerical modelling of a conventional tunnel excavation, Tunnelling and Underground Space Technology 108 (2021) 103723. doi:https://doi.org/10.1016/j.tust.2020.103723.

[44] S. Providakis, C. D. Rogers, D. N. Chapman, Predictions of settlement risk induced by tunnelling using BIM and 3D visualization tools, Tunnelling and Underground Space Technology 92 (2019) 103049. doi:https://doi.org/10.1016/j.tust.2019.103049.

[45] D. Potts, T. Addenbrooke, A structure's influence on tunnellinginduced ground movements, Proceedings of the Institution of Civil Engineers: Geotechnical Engineering 125 (2) (1997) 109–125. doi:10.1680/igeng.1997.29233.

[46] M. Hajjar, A. N. Hayati, M. M. Ahmadi, S. A. Sadrnejad, Longitudinal settlement profile in shallow tunnels in drained conditions, International Journal of Geomechanics 15 (6) (2015) 04014097. doi:10.1061/(ASCE)GM.1943-5622.0000447.

[47] X. Tan, A tool for optimal planning of urban tunnelling based on bim and effective 3d visualization.

[48] I.-B. Teodoru, EBBEF2p - a computer code for analyzing beams on elastic foundations, Intersections 6 (2009) 28–44.

[49] Autodesk, Autodesk Revit (2019).
URL `http://www.autodesk.co.uk/products/revit-family/`

[50] R. Peck, Deep excavations and tunnelling in soft ground, in: 7th International Conference on Soil Mechanics and Foundation Engineering Mexico City, 1969, pp. 225–290.

[51] P. O'Reilly Myles, B. New, Settlements above tunnels in the united kingdom-their magnitude and prediction, Tech. rep. (1982).

[52] C. Camós, O. Špačková, D. Straub, C. Molins, Probabilistic approach to assessing and monitoring settlements caused by tunneling, Tunnelling and Underground Space Technology 51 (2016) 313–325. doi:https://doi.org/10.1016/j.tust.2015.10.041.

[53] F. Pinto, A. J. Whittle, Ground movements due to shallow tunnels in soft ground. i: Analytical solutions, Journal of Geotechnical and Geoenvironmental Engineering 140 (4) (2014) 04013040. doi:10.1061/(ASCE)GT.1943-5606.0000948.

[54] A. Akhaveissy, The DSC Model for the Nonlinear Analysis of In-plane Loaded Masonry Structures, The Open Civil Engineering Journal 6 (11 2012). doi:10.2174/1874149501206010200.

[55] J. B. Burland, Settlement of buildings and associated damage.
URL `https://www.researchgate.net/publication/248646701`

[56] J. B. Burland, B. B. Broms, V. F. De Mello, Behaviour of foundations and structures, Building Research Establishment Garston, 1978.

[57] J. Ninić, G. Meschke, Model update and real-time steering of tunnel boring machines using simulation-based meta models, Tunnelling and Underground Space Technology 45 (2015) 138 – 152. doi:https://doi.org/10.1016/j.tust.2014.09.013.

[58] J. Kennedy, R. Eberhart, Particle swarm optimization (PSO), in: Proc. IEEE International Conference on Neural Networks, Perth, Australia, 1995, pp. 1942–1948.

[59] B. Ghiassi, G. Milani, Numerical modeling of masonry and historical structures - From theory to application, Woodhead Publishing, 2019.

[60] G. Giardina, M. A. Hendriks, J. G. Rots, Sensitivity study on tunnelling induced damage to a masonry façade, Engineering Structures 89 (2015) 111–129. doi:10.1016/j.engstruct.2015.01.042.

[61] M. Son, E. J. Cording, M.ASCE, Evaluation of building stiffness for building response analysis to excavation-induced ground movements (2007).

[62] A. Franza, S. Ritter, M. J. Dejong, Continuum solutions for tunnel–building interaction and a modified framework for deformation prediction, Géotechnique 70 (2) (2020) 108–122. doi:10.1680/jgeot.17.P.279.

[63] J. Zhao, M. DeJong, Three-dimensional probabilistic assessment of tunneling induced structural damage using monte-carlo method and hybrid finite element model, Computers and Geotechnics 154 (2023) 105122. doi:https://doi.org/10.1016/j.compgeo.2022.105122.

[64] S. Boudaa, S. Khalfallah, E. Bilotta, Static interaction analysis between beam and layered soil using a two-parameter elastic foundation, International Journal of Advanced Structural Engineering 11 (2019) 21–30.

[65] A. Turhan, A consistent Vlasov model for analysis of plates on elastic foundations using the finite element method, Texas Tech University, 1992.